The ribonuclease activity of SAMHD1 is required for HIV-1 restriction

Jeongmin Ryoo[1,2], **Jongsu Choi**[1,3], **Changhoon Oh**[1,2], **Sungchul Kim**[1,3], **Minji Seo**[1,3], **Seokyoung Kim**[1,3], **Daekwan Seo**[3], **Jongkyu Kim**[3,5], **Tommy E. White**[6], **Alberto Brandariz-Nunez**[6], **Felipe Diaz-Griffero**[6], **Cheol-Heui Yun**[7], **Joseph A. Hollenbaugh**[8], **Baek Kim**[8], **Daehyun Baek**[3,4,5], and **Kwangseog Ahn**[1,3]

Kwangseog Ahn: ksahn@snu.ac.kr

[1]Creative Research Initiative Center for Antigen Presentation, Seoul National University, Seoul 151-747, Republic of Korea

[2]Department of the Interdisciplinary Program in Genetic Engineering, Seoul National University, Seoul 151-747, Republic of Korea

[3]Department of Biological Sciences, Seoul National University, Seoul 151-747, Republic of Korea

[4]Bioinformatics Institute, Seoul National University, Seoul 151-747, Republic of Korea

[5]Center for RNA Research, Institute for Basic Science, Seoul 151-747, Republic of Korea

[6]Department of Microbiology and Immunology, Albert Einstein College of Medicine, Bronx, NY 10461, USA

[7]Department of Agricultural Biotechnology, Seoul National University, Seoul 151-921, Republic of Korea

[8]Center for Drug Discovery, Department of Pediatrics, Emory School of Medicine, Atlanta, Georgia, USA

Abstract

The HIV-1 restriction factor SAMHD1[1,2] is proposed to inhibit HIV-1 replication by depleting the intracellular dNTP pool[3-5]. However, the phosphorylation of SAMHD1 regulates its ability to restrict HIV-1 without decreasing cellular dNTP levels[6-8], which is not consistent with a role for SAMHD1 dNTPase activity in HIV-1 restriction. Here, we show that SAMHD1 possesses RNase activity and that the RNase but not the dNTPase function is essential for HIV-1 restriction. By enzymatically characterizing Aicardi-Goutières syndrome (AGS)-associated SAMHD1 mutations and mutations in the allosteric dGTP-binding site of SAMHD1, we identify SAMHD1 mutants that are RNase-positive but dNTPase-negative (SAMHD1$_{D137N}$) or RNase-negative but dNTPase-positive (SAMHD1$_{Q548A}$). The allosteric mutant SAMHD1$_{D137N}$ is able to restrict HIV-1 infection, whereas the AGS mutant SAMHD1$_{Q548A}$ is defective for HIV-1 restriction. SAMHD1

associates with HIV-1 RNA and degrades it during the early phases of infection. *SAMHD1* silencing in macrophages and CD4^{+} T cells from healthy donors increases HIV-1 RNA stability, rendering the cells permissive for HIV-1 infection. Furthermore, the phosphorylation of SAMHD1 at T592 negatively regulates its RNase activity *in vivo* and impedes HIV-1 restriction. Our results reveal that the RNase activity of SAMHD1 is responsible for preventing HIV-1 infection by directly degrading the HIV-1 RNA.

Keywords

SAMHD1; ribonuclease; HIV-1 restriction factor; HIV-1 genomic RNA; Aicardi-Goutières syndrome

Mutations in *SAMHD1* cause Aicardi-Goutières syndrome (AGS), which is a genetic autoimmune disorder that mimics a congenital viral infection[9,10]. SAMHD1 is a myeloid cell-specific HIV-1 restriction factor that is counteracted by Vpx[1,2]. SAMHD1 possesses a dGTP-dependent dNTPase activity[11,12], and studies have proposed that SAMHD1 blocks HIV-1 infection by depleting the intracellular dNTP pool[3-5]. Contrary to the proposed role for dNTPase activity in SAMHD1-mediated restriction of HIV-1, the phosphorylation of SAMHD1 regulates the ability of this enzyme to restrict HIV-1 infection but does not alter the cellular dNTP levels[6-8]. In addition, SAMHD1 is a nucleic acid binding protein[13-15] and exhibits a nuclease activity *in vitro* against diverse nucleic acid substrates[16]. Although the physiological relevance of SAMHD1 nuclease activity remains unknown, the aforementioned characteristics suggest that SAMHD1 might bind to HIV-1 RNA and degrade this RNA or reverse transcription intermediates.

In contrast to Beloglazova et al.[16], other studies have not observed SAMHD1 nuclease activity[11-13]; therefore, we tested whether SAMHD1 possesses nuclease activity. We incubated full-length, wild-type human SAMHD1 (SAMHD1$_{WT}$) (Supplementary Fig. 1) with various types of nucleic acid substrates. SAMHD1$_{WT}$ hydrolyzed both 20- and 30-mer single-stranded RNAs (ssRNA) processively (Fig. 1a and Supplementary Fig. 2a). No nuclease activity was detected on double-stranded RNA (dsRNA), single-stranded DNA (ssDNA), double-stranded DNA (dsDNA), and RNA-DNA hybrid substrates, whereas these substrates were digested by positive control nucleases (Supplementary Fig. 2b–e) (substrate sequences are shown in Supplementary Table 1). A previous study[16] observed that SAMHD1 degrades ssRNA, ssDNA, and RNA in DNA-RNA hybrids; however, we observed that only ssRNAs, including *in vitro*-HIV-1 transcripts (Supplementary Fig. 3), were sensitive to SAMHD1 digestion when the experiments were repeated using the various types of 40-mer nucleic acid substrates described by Beloglazova et al.[16] (Supplementary Fig. 4). These discrepancies might be due to differences in assay conditions or protein purification procedures; however, our results are consistent with the observation of Beloglazova et al.[16] that SAMHD1 cleaves ssRNAs *in vitro*. The degradation of ssRNA by SAMHD1 required Mg^{2+} (Supplementary Fig. 5) and correlated with the presence of the SAMHD1$_{WT}$ protein across chromatographic fractions (Supplementary Fig. 6). Considering the preferential binding of SAMHD1 to ssRNA compared with ssDNA[13,15] and no

interaction between endogenous SAMHD1 and dsRNA, dsDNA or RNA-DNA hybrids[15], we concluded that SAMHD1 is an RNase that digests ssRNA.

Unlike dNTPase activity, RNase activity does not require the cofactor dGTP (Fig. 1a); therefore, we proposed that these two catalytic functions of SAMHD1 might be physically separable. We characterized AGS-associated SAMHD1 mutations and mutations near the allosteric sites for defects in RNase or dNTPase activity and identified several point mutations that caused loss of function. Mutations at residues 207 and 311 in the catalytic site abolished both RNase and dNTPase activities (Figs. 1b,c). The allosteric mutant SAMHD1$_{D137N}$ had no effect on the RNase activity but did abolish the dNTPase activity (Figs. 1b,c). The AGS mutant SAMHD1$_{Q548A}$ showed the opposite phenotype. Unlike the processive degradation seen in SAMHD1$_{WT}$ and SAMHD1$_{D137N}$, a mutation at Q548 caused the enzyme to digest ssRNA in a distributive manner featured by accumulation of intermediate size fragments (16∼19-mer) (Fig. 1d). Considering that a shift from a processive to distributive degradation often occurs under the conditions that decrease the affinity of exonuclease to the substrates[17], this switch in mode may be because of a lowered affinity of SAMHD1$_{Q548A}$ to ssRNA. Indeed, recent studies have shown that SAMHD1$_{Q548A}$ exhibits impaired ssRNA-binding[15,16]. Notably, dGTP inhibited the RNase activity of SAMHD1 on ssRNA substrates, and this inhibition correlated with a shift from a processive to a distributive hydrolysis (Fig. 1e), suggesting that dGTP interferes with the binding of ssRNA substrates to SAMHD1. The identification of the SAMHD1 mutants that retain only one of two enzymatic activities enabled us to determine the discrete contribution of SAMHD1 RNase activity to HIV-1 restriction. For this analysis, we stably expressed SAMHD1 mutants in U937 pro-monocytic cells, which do not express endogenous SAMHD1[1,3,6,7] (Supplementary Fig. 7). Consistent with *in vitro* data (Fig. 1c,d), SAMHD1$_{D207N}$, SAMHD1$_{D311A}$, and SAMHD1$_{D137N}$ did not reduce the intracellular levels of dNTPs, whereas SAMHD1$_{Q548A}$ decreased the cellular levels of dNTPs (Fig. 1f). As expected, SAMHD1$_{D207N}$ and SAMHD1$_{D311A}$ did not restrict HIV-1 infection. Notably, SAMHD1$_{D137N}$ restricted HIV-1 infection to nearly the same extent as SAMHD1$_{WT}$. SAMHD1$_{Q548A}$ was unable to block HIV-1 restriction despite its ability to decrease the cellular levels of dNTPs (Fig. 1g). These data suggest that the RNase but not the dNTPase function of SAMHD1 is essential for HIV-1 restriction.

The quantification of viral cDNA intermediates showed that SAMHD1$_{D137N}$ inhibited the synthesis of both the early and late viral cDNA products (Supplementary Fig. 8), indicating that SAMHD1 RNase functions at the early step of HIV-1 reverse transcription. Thus, we tested whether SAMHD1 RNase activity affects HIV-1 RNA levels. HIV-1 RNA was significantly reduced in cells expressing SAMHD1$_{WT}$ or SAMHD1$_{D137N}$ 3 and 6 h post-infection (hpi) (Fig. 2a), but SAMHD1$_{D207N}$, SAMHD1$_{D311A}$, and SAMHD1$_{Q548A}$ did not reduce the HIV-1 RNA level; these results were consistent with FACS analyses (Fig. 1g). To exclude primer-specificity bias, 12 pairs of primers spanning the entire HIV-1 genomic RNA (Supplementary Table 2) were used to amplify fragments from HIV-1-infected cells. The HIV-1 RNA level in SAMHD1$_{WT}$-expressing cells was distinctly lower compared with the mock-transfected cells (Supplementary Fig. 9). To exclude the effect of the viral reverse transcriptase RNase H activity on the HIV-1 RNA level, we used RNase H-defective HIV-1

(HIV-1_{D443N}) in which the Asp-443 of reverse transcriptase was mutated to Asn (D443N)[18]. The HIV-1_{D443N} RNA level was lower in SAMHD1$_{WT}$-expressing cells compared with mock-transfected cells (Fig. 2b), indicating that SAMHD1 can degrade HIV-1 RNA in the absence of reverse transcription.

RNA-Seq analysis also confirmed the degradation of HIV-1 RNA by SAMHD1. At 3 hpi, the relative read count of HIV-1 RNA in SAMHD1$_{WT}$ and SAMHD1$_{D137N}$-expressing cells was lower than that in mock-transfected or SAMHD1$_{D207N}$-expressing cells despite the considerable reduction of HIV-1 RNA levels in all cell types compared with the levels observed at 1 hpi (Figs. 2c,d). shRNA-mediated knockdown of SAMHD1 or Vpx-mediated degradation of endogenous SAMHD1 in THP-1 cells also caused an approximately four-fold increase in the HIV-1 RNA level (Fig. 2e). RNA immunoprecipitation (RIP) analysis[19] revealed that a significant enrichment of HIV-1 RNA was observed in the immunoprecipitates from cells expressing SAMHD1$_{WT}$-HA. The HIV-1 RNA enrichment was more pronounced for the SAMHD1$_{D207N}$-HA catalytic mutant with an approximately eight-fold increase (Fig. 2f), suggesting that SAMHD1 associates with HIV-1 genomic RNA. In contrast, interaction of SAMHD1$_{Q548A}$-HA with HIV-1 RNA was significantly reduced when compared with the SAMHD1$_{WT}$-HA (Fig. 2f), supporting that impaired binding of SAMHD1$_{Q548A}$-HA to HIV-1 RNA accounts for its inability to cleave short ssRNA and HIV-1 RNA (Figs. 1d and 2a).

Next, we analyzed the role of SAMHD1 RNase in degrading HIV-1 RNA in primary human monocyte-derived macrophages (MDMs) and CD4+ T cells. The differentiation of MDM and activation state of CD4+ T cells were analyzed by monitoring their surface markers (Supplementary Figs. 10 and 11). *SAMHD1* silencing in MDMs markedly reduced the cellular SAMHD1 levels (Fig. 3a, left) and rendered MDMs more permissive to HIV-1 infection (Fig. 3a and Supplementary Fig. 12), a result that is correlated with the increased stability of HIV-1 RNA. The enhancement of HIV-1 RNA stability ranged from approximately two to four-fold, depending on the donor (Fig. 3a, middle). Similar to the results obtained using MDMs, *SAMHD1* silencing in resting CD4+ T cells increased the infectivity of HIV-1 (Fig. 3b and Supplementary Fig. 12). In these cells, increased HIV-1 RNA stability was observed 3 hpi (Fig. 3b, middle). The degradation of SAMHD1 by Vpx could also stabilize the viral RNAs of HIV-1 and HIV-1_{D443N} in resting CD4+ T cells (Fig. 3c). These results show that the antiviral activity of SAMHD1 correlates with its RNase activity in primary MDMs and resting CD4+ T cells. Biochemical fractionation revealed that SAMHD1 is localized in both the cytoplasm and nucleus of MDMs and monocytes (Supplementary Fig. 13), which is consistent with previous observations[4,13]. Considering that cytoplasmic SAMHD1 can block HIV-1 infection[20,21], these data suggest that after virus uncoating, SAMHD1 associates with and degrades HIV-1 RNA in the cytoplasm.

The phosphorylation of SAMHD1 at T592 causes the loss of HIV-1 restriction without decreasing cellular dNTP levels[6-8]. We tested whether the phosphorylation of SAMHD1 affects its RNase activity in HIV-1 restriction. In PMA-treated U937 cells where SAMHD1$_{WT}$ is not phosphorylated on T592[6,7], SAMHD1$_{WT}$ blocked HIV-1 infection. In contrast, SAMHD1$_{T592D}$ containing the phosphomimetic D residue was unable to inhibit HIV-1 infection (Fig. 4a), confirming previous results[6]. Notably, the stability of HIV-1

RNA was enhanced by three to four-fold in cells expressing SAMHD1$_{T592D}$ compared with cells expressing SAMHD1$_{WT}$ (Fig. 4b). In contrast to this *in vivo* observation, the recombinant SAMHD1$_{T592D}$ protein was as effective as the SAMHD1$_{WT}$ and the nonphosphorable SAMHD1$_{T592V}$ in degrading ssRNA substrates *in vitro* (Fig. 4c). RIP analysis revealed that SAMHD1$_{WT}$ and SAMHD1$_{T592D}$ bound to HIV-1 genomic RNA with similar affinities, indicating that phosphorylation of SAMHD1 T592 does not interfere with substrate binding (Fig. 4d). The discrepancy between the *in vivo* and *in vitro* RNase activities suggests that the phosphorylation of SAMHD1 might promote the recruitment of cellular factors that negatively regulate its RNase activity or interfere with the interaction of SAMHD1 with unidentified cofactors. Our results reveal that the phosphorylation of SAMHD1 at T592 is a mechanism that negatively regulates its RNase activity *in vivo* and impedes HIV-1 restriction.

The crystal structure of SAMHD1 reveals that this protein is dimeric and indicates a structural basis for allosteric activation of catalytic activity against dNTPs by dGTP binding[11]. By contrast, recent studies have demonstrated that SAMHD1 oligomerizes in a dGTP-dependent manner up to a tetramer and that the tetramerization of SAMHD1 is required for its dNTPase and anti-HIV-1 activities[22-24]. Notably, SAMHD1 with a mutation at the allosteric dGTP-binding site D137 did not undergo oligomerization and was mostly monomeric in the presence of dGTP[22]. The mutation of D137 (SAMHD1$_{D137N}$) abolishes SAMHD1 dNTPase but not RNase activity (Fig. 1), indicating that unlike the dNTPase activity, the tetramerization of SAMHD1 is not necessary for its RNase activity. Based on previous data and our results, we propose that SAMHD1 is a dual-function enzyme whose mutually exclusive and predominant activities depend on the dGTP pool. At low dGTP levels, SAMHD1 exists as monomers or dimers that harbor active RNase but not dNTPase activity, enabling HIV-1 restriction through the cleavage of HIV-1 RNA. At high dGTP levels, SAMHD1 tetramerizes, yielding an enzyme with an inactive RNase but active dNTPase function (Fig. 4e). An alternative but not mutually exclusive possibility is that the ssRNA and dNTP substrates might compete with each other for a common active site on the enzyme. dGTP is both a substrate and an activator of the SAMHD1 dNTPase function[11,12]; this model is consistent with the observations that high levels of dGTP impair the binding of SAMHD1 to nucleic acid substrates *in vitro*[6,16], that the switch from a processive to distributive degradation of ssRNA in dGTP-dependent manner (Fig. 1e) is indicative of competitive inhibition of ssRNA-binding by dGTP, and that mutations in the catalytic site abolish both RNase and dNTPase activities (Fig. 1). In this respect, the partial alleviation of SAMHD1-mediated HIV-1 restriction by the addition of exogenous dNs[3] might be an indirect consequence of impaired RNA substrate binding by increased dGTP levels. These two hypotheses may also explain why SAMHD1 blocks HIV-1 infection only in non-cycling cells, such as DCs and macrophages with low dNTP levels[1], but not in cycling cells with high dNTP levels[4,6,25]. Another explanation might be that in non-cycling cells, dNTP limitation would slow down reverse transcription, and this could allow a sufficient time window for the action of SAMHD1 RNase against HIV-1 RNA. The identification of SAMHD1 as an RNase suggests that SAMHD1 is involved in nucleic acid metabolism related to the prevention of an innate immune response; therefore, our results provide insight into the mechanisms underlying HIV-1 restriction and the pathogenesis of AGS.

Online Methods

Ethics statement

Adult blood samples were anonymously provided by the Blood Center of the Korean Red Cross, Seoul, under the approval of the Institutional Review Board of Korean Red Cross with consent for research use. Written informed consent was obtained from the blood donors with the approval of the Ethics Committee of the Korean Red Cross. Experiments involving human blood were approved by the Institutional Review Board at Seoul National University (SNUIRB No. E1304-001-023).

Plasmids

Full-length human SAMHD1 was amplified by PCR from cDNA generated by the reverse transcription of RNA from HeLa cells, and the PCR product was inserted into a pGEX-4T-1 vector and a pMSCV-puro vector. The $SAMHD1_{D207N}$, $SAMHD1_{D311A}$, $SAMHD1_{D137N}$ and $SAMHD1_{Q548A}$ mutants were generated using the nPfu-forte DNA Polymerase Kit (Enzynomics). Retroviral vectors encoding the wild-type or T592 phosphorylation variants SAMHD1 were described previously[6]. HIV-1-GFP, pLai envGFP3, and HCMV-VSV-G were described previously[27].

Protein expression and purification

The GST-tagged, full-length, human SAMHD1 proteins (GST-SAMHD1) were expressed in *E. coli* Rosetta (λDE3) (Novagen). The Rosetta cells were grown in Terrific broth containing ampicillin ($100\ \mu g\ ml^{-1}$) at 37 °C to an optical density $(OD)_{600}$ of 2.0, and the cells were rapidly cooled on ice to 16 °C. After induction with 0.1 mM isopropyl-β-D-thiogalactopyranoside (IPTG; Ducheba), the cells were allowed to grow for 16 h at 16 °C. The *E. coli* pellet containing the GST fusion protein was lysed with PBS, and the protein was purified using glutathione-Sepharose column chromatography, as previously described [28].

Immunoprecipitation for *in vitro* nuclease assay

Cell pellets derived from the stable U937 cell lines expressing mock and HA-tagged SAMHD1 were resuspended in lysis buffer (25 mM Tris-HCl, pH 7.5, 100 mM KCl, 1 mM DTT, 2 mM EDTA, 0.5 mM PMSF, 0.05% NP-40) containing an RNase inhibitor and were incubated for 30 min on ice, sonicated, and centrifuged at $13,000 \times g$ at 4 °C for 30 min. Monoclonal mouse antibody to HA coupled to protein A–agarose beads (Sigma) was added, and precipitates were washed twice with buffer A (500 mM NaCl, 10 mM Tris-HCl, pH 7.5, 0.05% NP-40, RNase inhibitor) and twice with buffer B (150 mM NaCl, 10 mM Tris-HCl, pH 7.5, 0.05% NP-40, RNase inhibitor). Cell extracts were incubated with the antibody-coupled beads for 1 h at 4 °C. Immunoprecipitates were washed five times with buffer B followed by elution with HA-peptide.

Preparation of DNA and RNA substrates

Fragments of the HIV-1 5′ LTR, *gag*, and 3′ LTR were transcribed *in vitro* using T7 RNA polymerase (Enzynomics). The transcripts were purified using denaturing polyacrylamide

gel electrophoresis (PAGE; 5% polyacrylamide, 8 M urea). Synthetic DNA and RNA oligonucleotides were 5′-end labeled with ^{32}P using T4 polynucleotide kinase and [γ-^{32}P]ATP. The nucleotides were precipitated by the addition of 3 M ammonium acetate and 100% (vol/vol) ethanol. The nucleotides pellets were washed with 75% ethanol, dried and resuspended in 10 mM Tris-Cl (pH 7.8) containing 1 mM EDTA. The synthetic dsDNAs and dsRNAs (Supplementary Table 1) were prepared by annealing the oligonucleotides.

In vitro nuclease assay

Assays were performed in 20-μl reaction mixtures containing PBS supplemented with 5 mM $MgCl_2$, 2 mM DTT, 10% glycerol, 0.01% NP-40, ^{32}P-labeled nucleic acid substrates, and purified recombinant proteins (150 nM) or immunoprecipitated proteins at 37 °C for the indicated times. The reactions were stopped by the addition of an equal volume of formamide loading buffer and then boiled. The products were separated in 15% polyacrylamide gels containing 8 M urea and buffered with $0.5 \times$ Tris-borate-EDTA (TBE) and then analyzed by autoradiography using a phosphorimager (BAS2500, Fujifilm).

dGTP-triphosphohydrolase assay

An enzymatic assay based on thin layer chromatography was performed as described previously[3]. The purified recombinant protein (1 μM) was incubated in 50 mM Tris-HCl (pH 8.0), 20 mM KCl, 5 mM $MgCl_2$, 0.1 μCi [α-^{32}P]dGTP, and 200 μM cold dGTP for 3 h at 37 °C. The reactions were stopped by heat-inactivation at 70 °C for 10 min. The reaction mixtures were spotted along with dGMP, dGDP, and dGTP standards onto polyethyleneimine (PEI)-cellulose plates (Sigma-Aldrich) and subsequently separated using a mobile phase of 1.2 M LiCl. After separation, the α-^{32}P-labeled reaction products were visualized using a phosphorimager, and the migration indicators were detected by UV-C (254 nm).

Cells and reagents

U937 and THP1 cells were cultured in RPMI 1640 supplemented with 10% fetal bovine serum (Hyclone), 2 mM GlutaMAX-I, 100 U ml^{-1} penicillin, and 100 μg ml^{-1} streptomycin (Invitrogen). 293T cells and Phoenix Ampho cells were cultured in DMEM supplemented as described for RPMI 1640. Stable U937 cells expressing SAMHD1 proteins were obtained by retroviral infection. The pMSCV-puro construct was used to transfect Phoenix Ampho cells using the calcium phosphate method. Two days later, the retrovirus-containing supernatant was used to transduce U937 cells by spin infection with 8 μg ml^{-1} polybrene. The transduced cells were selected in 1 μg ml^{-1} puromycin. Peripheral blood mononuclear cells (PBMCs) were obtained from human blood by density gradient centrifugation using Ficoll-Paque Plus™ (Amersham Healthcare). Monocytes were isolated from the PBMCs using a magnetic bead-based positive selection kit (IMag™) and anti-human CD14 beads (cat. 557769, BD Biosciences). This procedure routinely yielded over 90% pure CD14-positive cells, as verified by flow cytometry. MDMs were obtained from monocytes by culturing the cells for 3 d with GM-CSF (10 ng ml^{-1}) and M-CSF (20 ng ml^{-1}). The differentiation state of CD14^{+} cells was analyzed by monitoring the differentiation markers CD71 (cat. 555536, BD Biosciences), CD80 (cat. 557226, BD Biosciences), and CD86 (cat.

555657, BD Biosciences). CD4$^+$ T cells were isolated from the PBMCs using a magnetic bead-based positive selection kit (IMag™) and anti-human CD4 beads (cat. 557767, BD Biosciences). T cells were activated, and post-activation resting T cells were obtained as previously described[4]. Resting CD4$^+$ T cells (2×10^6 cells ml^{-1}) were treated overnight with PHA-L (2 mg ml^{-1}). The next day, the medium was exchanged and cells were incubated in RPMI medium with 20 IU ml^{-1} IL-2 for 3 d. Activated CD4$^+$ T cells were electroporated with SAMHD1-specific siRNA or non-specific siRNAs. The siRNA-treated cells were cultivated in RPMI medium with gradually reducing concentrations of IL-2. The activation state of CD4$^+$ T cells was analyzed by monitoring the surface expression of the activation markers CD25 (cat. 555434, BD Biosciences) and CD69 (cat. 555533, BD Biosciences). The experimental design for the time course analysis of MDMs and CD4$^+$ T cells is shown in Supplementary Figs. 10 and 11.

RNA interference

siRNA targeting *SAMHD1* was purchased from Dharmacon. MDMs and CD4$^+$ T cells (2×10^6 cells) were electroporated in 100-μl reactions with siRNA (10 nM) using the Neon Transfection System (Invitrogen). Transfections with ON-TARGETplus Non-targeting pool (Dharmacon) were performed in parallel as a negative control. The MDMs and CD4$^+$ T cells were pulsed once each for 20 ms at 2,150 and 2,100 volts, respectively.

Viruses and VLP production

293T cells were transfected with 10 μg of HIV-1-GFP, HIV-1$_{D443N}$-GFP or pLai envGFP3 and 2 μg of HCMV-VSV-G using the calcium phosphate method. Vpx-containing and control VLPs were generated by the transfection of 293T cells with pSIV3+ or pSIV3+ *vpx*. Culture supernatants were collected and filtered (0.45 μm) 48 h after transfection. U937 cells (0.5×10^6 cells ml^{-1}) were seeded in 12-well plates and differentiated for 20 h in PMA (30 ng ml^{-1}). The cells were infected with 100 ng of pseudotyped viruses for 2 h. The cells were then washed and cultured for 48 h. Infected cells were analyzed by flow cytometry or qRT-PCR.

Quantitative real-time PCR

VSV-G-pseudotyped HIV-1-GFP-infected cells were harvested at various time points, and DNA was isolated using the QIAamp Blood DNA Minikit (Qiagen). qPCR was performed with the iCycler iQ real-time PCR detection system (BioRad) using HIV-1-specific primers: R/U5 (forward, GCCTCAATAAAGCTTGCCTTGA; reverse, TGACTAAAAGGGTCTGAGGGATCT) and U5/ψ (forward, TGTGTGCCCGTCTGTTGTGT; reverse, GAGTCCTGCGTCGAGAGATC). RNA isolation from HIV-1-GFP-infected cells was performed at various time points according to the manufacturer's instructions (Invitrogen). One microgram of RNA was treated with DNase I prior to qPCR analysis and isolated by phenol:chloroform extraction. The data were normalized to an internal control gene, *MDM2* or *β-actin*. The purified RNA was reverse transcribed using random primers, and real-time PCR was performed with the iCycler iQ real-time PCR detection system (BioRad) using HIV-1-specific primers: *gag* (forward, CTAGAACGATTCGCAGTTAATCCT; reverse, CTATCCTTTGA

TGCACACAATAGAG) and *egfp* (forward, CAACAGCCACAACGTCTATATCATG; reverse, ATGTTGTGGCGGATCTTGAAG).

RNA-Seq Analysis

Total RNA was extracted from mock- and SAMHD1-expressing U937 cells uninfected or infected with HIV-1 using TRIzol reagent (Invitrogen) by manufacturer's instruction followed by addition of spike-in poly(A)-tailed RNA (GeneChip Eukaryotic Poly-A RNA control Kit, Affymetrix) to reduce background noise and allow comparison between samples. After ribosomal RNA depletion using Epicentre's Ribo-Zero™ Kits, RNA was fragmented using RNA fragmentation reagent (Ambion). After dephosphorylation by Antarctic phosphatase (NEB), 5′ end of fragmented and dephosphorylated RNA was phospho-labeled using [γ-^{32}P]ATP and T4 polynucleotide kinase (TaKaRa). 35–60 nucleotide RNA was extracted in a polyacrylamide, 7 M urea, TBE gel. 3′ adaptor (5′/rApp/ TGGAATTCTCGGGTGCCAAGG/ddC/-3′, IDT) was ligated using T4 RNA ligase truncated K227Q (NEB) followed by ligation of 5′ adaptor (5′ Solexa linker, 100-M; 5′rGrUrUrCrArGrArGrUrUrCrUrArCrArGrUrCrCrGrArCrGrA rUrC-3′, IDT) using T4 RNA ligase (TaKaRa). The 5′ and 3′ adaptor-ligated RNA was reverse transcribed using RNA RT Primer (RTP; 5′GCCTTGGCACCCGAGAATTCCA-3′, IDT) and SuperScript™ III reverse transcriptase (Invitrogen). Each sample was amplified by PCR using Phusion polymerase (Thermo Scientific), 5′ end Illumina RNA PCR Primer (RP1) and 3′ end Illumina RNA PCR Primer (Index 1–12). RNA-Seq library was sequenced with 51-bp single-end sequencing in an Illumina HiSeq2500 sequencer. Illumina standard pipeline and software-CASAVA were employed for processing of raw imaging, base calling and generating FASTQ sequence reads. Before aligning reads to the reference sequences, we filtered low quality reads, adapter-containing sequences, and artifact reads using in house software and FASTX-Toolkit (FASTQ/A short-reads pre-processing tools, hannonlab.cshl.edu/fastx toolkit). The read sequences were then aligned to the UCSC hg19 human reference genome and HIV-1 NL4-3 genome using bowtie2-2.1.0[29]. The abundance of transcripts was measured as the score of RPKM (Reads Per Kilobase of exon model per Million mapped reads). We applied spike-in normalization to all 12 samples to reduce variations across samples.

RNA immunoprecipitation (RIP)

The RNA immunoprecipitation protocol[19] was adapted to analyze the interactions between SAMHD1 and HIV-1-GFP genomic RNA. HIV-1-GFP-infected cells were cross-linked by 1% formaldehyde for 10 min at room temperature. The crosslinking reaction was stopped by addition of glycine (1 M, pH 7.0) to a final concentration of 0.25 M followed by incubation at room temperature for 5 min. The cells were washed with ice-cold PBS and resuspended in RIPA buffer (50 mM Tris-HCl, pH 7.4, 1% NP40, 0.5% sodium deoxycholate, 0.05% SDS, 1 mM EDTA, 150 mM NaCl) containing protease inhibitors and an RNase inhibitor. The cell suspension was sonicated and centrifuged for 10 min at 9,000 × *g*, and the resulting supernatant was pre-cleared by incubation with protein G-agarose beads. The pre-cleared supernatant was incubated with anti-HA (A2095, Sigma) or anti-Flag antibody-conjugated beads (A2220, Sigma) for 2 h at 4 °C. The beads were washed with RIPA buffer and resuspended with reversal buffer (50 mM Tris-HCl, pH 7.0, 5 mM EDTA, 10 mM DTT, 1%

SDS) followed by an incubation for 45 min at 70 °C to reverse the crosslinks. The immunoprecipitated RNAs were isolated according to the manufacturer's protocol (Invitrogen).

Cell fractionation

For nuclear-cytoplasmic fractionation, monocytes and MDMs were washed in cold PBS and resuspended with lysis buffer (10 mM HEPES, pH 7.9, 0.1 mM EDTA, 2 mM MgCl$_2$, 0.1 mM EGTA, 10 mM KCl, 0.1 mM DTT, and 0.5 mM PMSF). NP-40 was added to obtain a final concentration of 1% and mixed by gentle inversion. The cytoplasmic extracts were separated from intact nuclei by low-speed centrifugation at 4 °C and $1400 \times g$ for 30 s. The nuclear pellet was resuspended in buffer (20 mM HEPES, pH 7.9, 0.1 mM EDTA, 0.1 mM EGTA, 0.4 M NaCl, 1 mM DTT, and 1 mM PMSF). The nuclear and cytoplasmic fractions were analyzed by immunoblotting.

Supplementary Material

Refer to Web version on PubMed Central for supplementary material.

Acknowledgments

References

1. Laguette N, et al. SAMHD1 is the dendritic- and myeloid-cell-specific HIV-1 restriction factor counteracted by Vpx. Nature. 2011; 474:654–657. [PubMed: 21613998]

2. Hrecka K, et al. Vpx relieves inhibition of HIV-1 infection of macrophages mediated by the SAMHD1 protein. Nature. 2011; 474:658–661. [PubMed: 21720370]

3. Lahouassa H, et al. SAMHD1 restricts the replication of human immunodeficiency virus type 1 by depleting the intracellular pool of deoxynucleoside triphosphates. Nat Immunol. 2012; 13:223–228. [PubMed: 22327569]

4. Baldauf HM, et al. SAMHD1 restricts HIV-1 infection in resting CD4(+) T cells. Nat Med. 2012; 18:1682–1689. [PubMed: 22972397]

5. St Gelais C, et al. SAMHD1 restricts HIV-1 infection in dendritic cells (DCs) by dNTP depletion, but its expression in DCs and primary CD4+ T-lymphocytes cannot be upregulated by interferons. Retrovirology. 2012; 9:105. [PubMed: 23231760]

6. White TE, et al. The Retroviral Restriction Ability of SAMHD1, but Not Its Deoxynucleotide Triphosphohydrolase Activity, Is Regulated by Phosphorylation. Cell Host Microbe. 2013; 13:441–451. [PubMed: 23601106]

7. Cribier A, Descours B, Valadao AL, Laguette N, Benkirane M. Phosphorylation of SAMHD1 by Cyclin A2/CDK1 Regulates Its Restriction Activity toward HIV-1. Cell Rep. 2013; 3:1036–1043. [PubMed: 23602554]

8. Welbourn S, Dutta SM, Semmes OJ, Strebel K. Restriction of virus infection but not catalytic dNTPase activity is regulated by phosphorylation of SAMHD1. J Virol. 2013; 87:11516–11524. [PubMed: 23966382]

9. Rice GI, et al. Mutations involved in Aicardi-Goutieres syndrome implicate SAMHD1 as regulator of the innate immune response. Nat Genet. 2009; 41:829–832. [PubMed: 19525956]

10. Crow YJ, Rehwinkel J. Aicardi-Goutieres syndrome and related phenotypes: linking nucleic acid metabolism with autoimmunity. Hum Mol Genet. 2009; 18:R130–136. [PubMed: 19808788]

11. Goldstone DC, et al. HIV-1 restriction factor SAMHD1 is a deoxynucleoside triphosphate triphosphohydrolase. Nature. 2011; 480:379–382. [PubMed: 22056990]

12. Powell RD, Holland PJ, Hollis T, Perrino FW. Aicardi-Goutieres syndrome gene and HIV-1 restriction factor SAMHD1 is a dGTP-regulated deoxynucleotide triphosphohydrolase. J Biol Chem. 2011; 286:43596–43600. [PubMed: 22069334]

13. Goncalves A, et al. SAMHD1 is a nucleic-acid binding protein that is mislocalized due to aicardi-goutieres syndrome-associated mutations. Hum Mutat. 2012; 33:1116–1122. [PubMed: 22461318]

14. White TE, et al. Contribution of SAM and HD domains to retroviral restriction mediated by human SAMHD1. Virology. 2013; 436:81–90. [PubMed: 23158101]

15. Tungler V, et al. Single-stranded nucleic acids promote SAMHD1 complex formation. J Mol Med (Berl). 2013

16. Beloglazova N, et al. Nuclease Activity of the Human SAMHD1 Protein Implicated in the Aicardi-Goutieres Syndrome and HIV-1 Restriction. J Biol Chem. 2013; 288:8101–8110. [PubMed: 23364794]

17. Barbas A, et al. New insights into the mechanism of RNA degradation by ribonuclease II: identification of the residue responsible for setting the RNase II end product. J Biol Chem. 2008; 283:13070–13076. [PubMed: 18337246]

18. Mizrahi V, Usdin MT, Harington A, Dudding LR. Site-directed mutagenesis of the conserved Asp-443 and Asp-498 carboxy-terminal residues of HIV-1 reverse transcriptase. Nucleic Acids Res. 1990; 18:5359–5363. [PubMed: 1699202]

19. Niranjanakumari S, Lasda E, Brazas R, Garcia-Blanco MA. Reversible cross-linking combined with immunoprecipitation to study RNA-protein interactions in vivo. Methods. 2002; 26:182–190. [PubMed: 12054895]

20. Hofmann H, et al. The Vpx lentiviral accessory protein targets SAMHD1 for degradation in the nucleus. J Virol. 2012; 86:12552–12560. [PubMed: 22973040]

21. Brandariz-Nunez A, et al. Role of SAMHD1 nuclear localization in restriction of HIV-1 and SIVmac. Retrovirology. 2012; 9:49. [PubMed: 22691373]

22. Yan J, et al. Tetramerization of SAMHD1 is required for biological activity and inhibition of HIV infection. J Biol Chem. 2013; 288:10406–10417. [PubMed: 23426366]

23. Ji X, et al. Mechanism of allosteric activation of SAMHD1 by dGTP. Nat Struct Mol Biol. 2013; 20:1304–1309. [PubMed: 24141705]

24. Zhu C, et al. Structural insight into dGTP-dependent activation of tetrameric SAMHD1 deoxynucleoside triphosphate triphosphohydrolase. Nat Commun. 2013; 4:2722. [PubMed: 24217394]

25. Descours B, et al. SAMHD1 restricts HIV-1 reverse transcription in quiescent CD4(+) T-cells. Retrovirology. 2012; 9:87. [PubMed: 23092122]

26. Diamond TL, et al. Macrophage tropism of HIV-1 depends on efficient cellular dNTP utilization by reverse transcriptase. J Biol Chem. 2004; 279:51545–51553. [PubMed: 15452123]

27. Manel N, et al. A cryptic sensor for HIV-1 activates antiviral innate immunity in dendritic cells. Nature. 2010; 467:214–217. [PubMed: 20829794]

28. Rohman M, Harrison-Lavoie KJ. Separation of copurifying GroEL from glutathione-S-transferase fusion proteins. Protein Expr Purif. 2000; 20:45–47. [PubMed: 11035949]

29. Langmead B, Salzberg SL. Fast gapped-read alignment with Bowtie 2. Nat Methods. 2012; 9:357–359. [PubMed: 22388286]
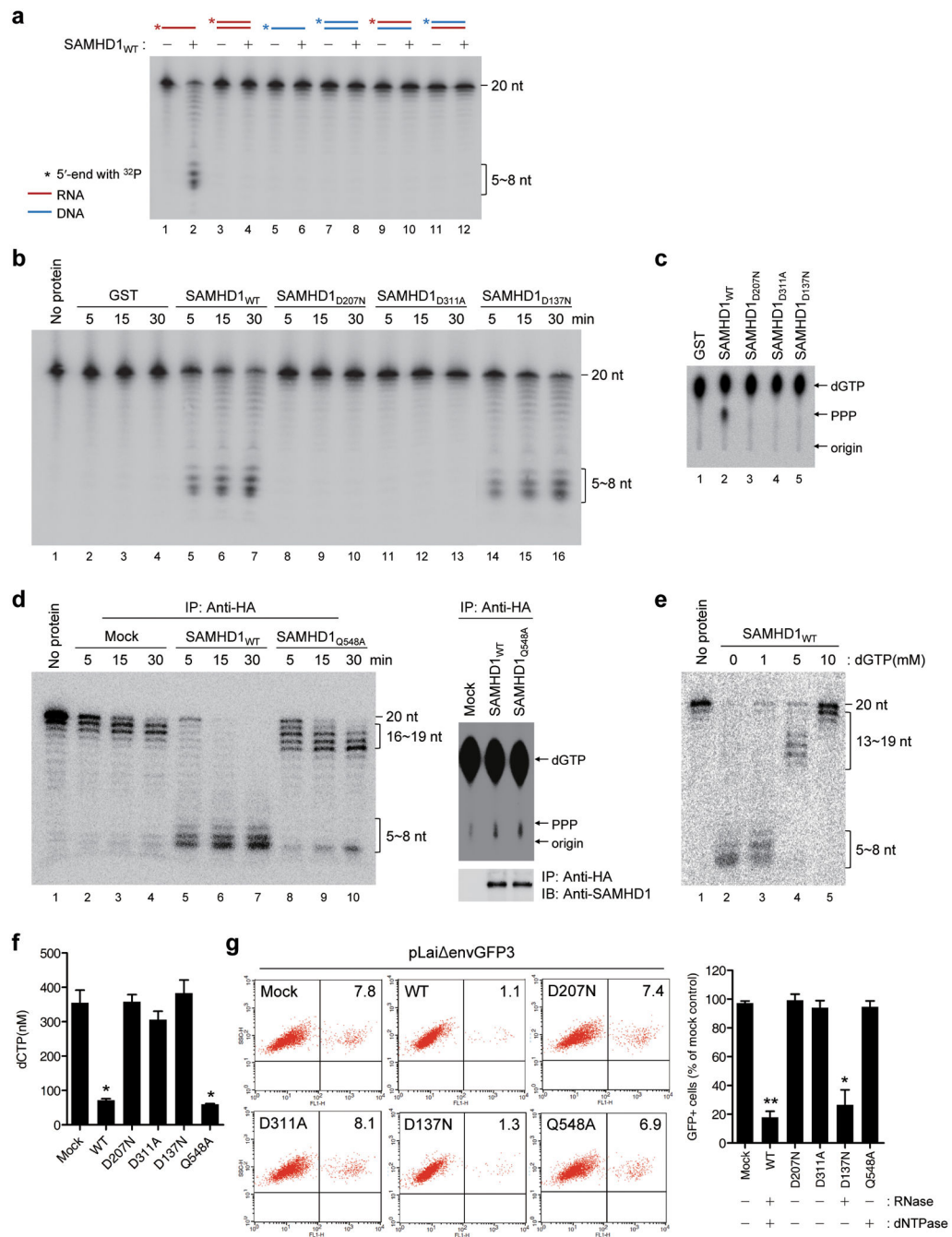
Figure 1.
The RNase but not the dNTPase function of SAMHD1 is required for HIV-1 restriction. (**a**) Purified GST-SAMHD1$_{WT}$ (150 nM) was incubated for 30 min at 37 °C with 5′-end ^{32}P labeled nucleic acid substrates (20-mer, 50 nM). The RNA and DNA are indicated by red and blue lines, respectively. (**b**) An RNase activity assay performed for SAMHD1 mutants as described in Fig. 1**a** using 20-mer ssRNA substrates. (**c**) A dGTP-triphosphohydrolase assay was performed for GST-SAMHD1 variants as described previously[3]. (**d**) The HA-tagged SAMHD1$_{WT}$ and SAMHD1$_{Q548A}$ proteins were purified from the PMA-

differentiated U937 cells using HA-antibody. An RNase and a dGTP triphosphohydrolase assays were performed as described above. (**e**) Inhibition of the SAMHD1 RNase activity by dGTP. The assay was performed as in **a** in the presence of dGTP. (**f**) The intracellular dNTP pools were measured in U937 cells stably expressing SAMHD1 variants as described[26]. (**g**) U937 cells stably expressing SAMHD1mutants were treated with PMA and infected by pLai envGFP3, a HIV-1-GFP reporter virus with the LAI backbone[27]. After 48 h, the percentages of GFP-positive cells were analyzed using flow cytometry. The percentage of GFP-positive cells was calculated relative to the number of GFP-positive mock-transfected cells. In **f** and **g**, the data are presented as the mean ± s.d. of triplicate independent experiments. (* and ** indicate significant differences compared with the mock-transfected control at $P < 0.05$ and $P < 0.001$, respectively, using the two-tailed Student's t test).
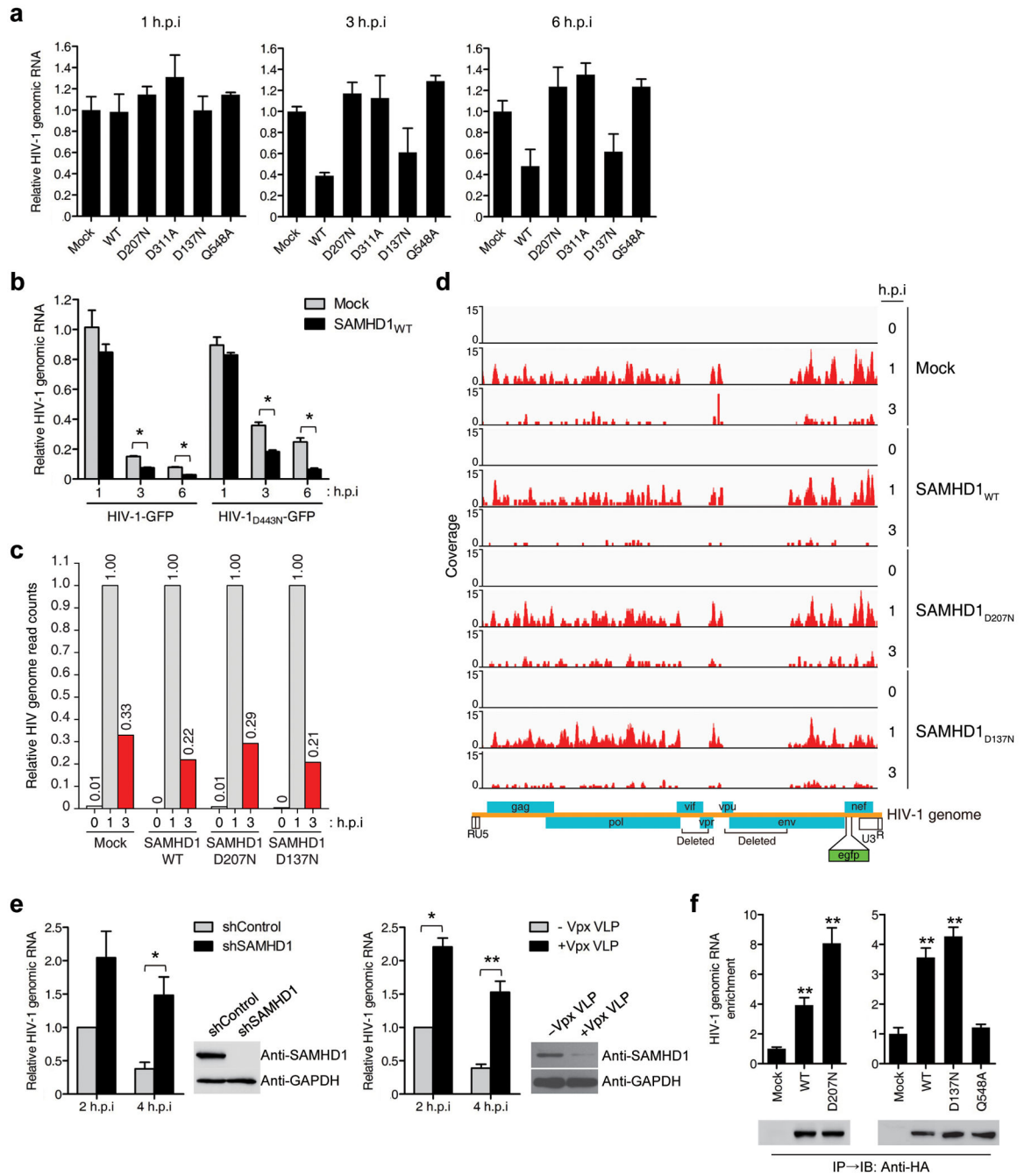
Figure 2.

SAMHD1 directly degrades HIV-1 RNA in human monocytic cells. (**a**) The total cellular RNA was extracted from SAMHD1-expressing, HIV-1-GFP-infected U937 cells. The HIV-1 RNA content was quantified by qRT-PCR using HIV-1 *gag*-specific primers. The data were normalized to an internal *β-actin*. (**b**) Mock- and SAMHD1$_{WT}$-expressing U937 cells were infected with HIV-1-GFP or HIV-1$_{D443N}$-GFP. The HIV-1 RNA content was quantified by qRT-PCR using HIV-1 *gfp*-specific primers. (**c**) Relative HIV-1 genome abundance in reads per kilobase per million mapped reads (RPKM) calculated from RNA-

Seq data. (**d**) Coverage of the RNA-Seq data across the HIV-1 genome in U937 cells expressing SAMHD1$_{WT}$, SAMHD1$_{D207N}$ and SAMHD1$_{D137N}$ after HIV-1-GFP infection. Data are representative of two independent experiments (**c**,**d**). (**e**) shRNA-mediated silencing of *SAMHD1* (left) or Vpx-mediated degradation of SAMHD1 (right) in THP-1 cells increases HIV-1 RNA stability. THP-1 cells expressing shRNAs, Vpx or negative control were treated with PMA for 24 h followed by infection with HIV-1-GFP. The total viral RNA was quantified by qRT-PCR at the indicated times post-infection. Knockdown efficiency was determined by immunoblot analysis. (**f**) Enrichment of HIV-1 genomic RNA in the SAMHD1 immunoprecipitates. U937 cells expressing HA-tagged SAMHD1 variants were infected for 90 min with HIV-1-GFP. The purified RNAs in the anti-HA immunoprecipitates were quantified by qRT-PCR using HIV-1 *gag*-specific primers. In **a, b, e,** and **f**, data are presented as the mean ± s.d. of triplicate independent experiments. (*$P < 0.05$ and **$P < 0.001$ versus Mock or shControl, two-tailed Student's t test).
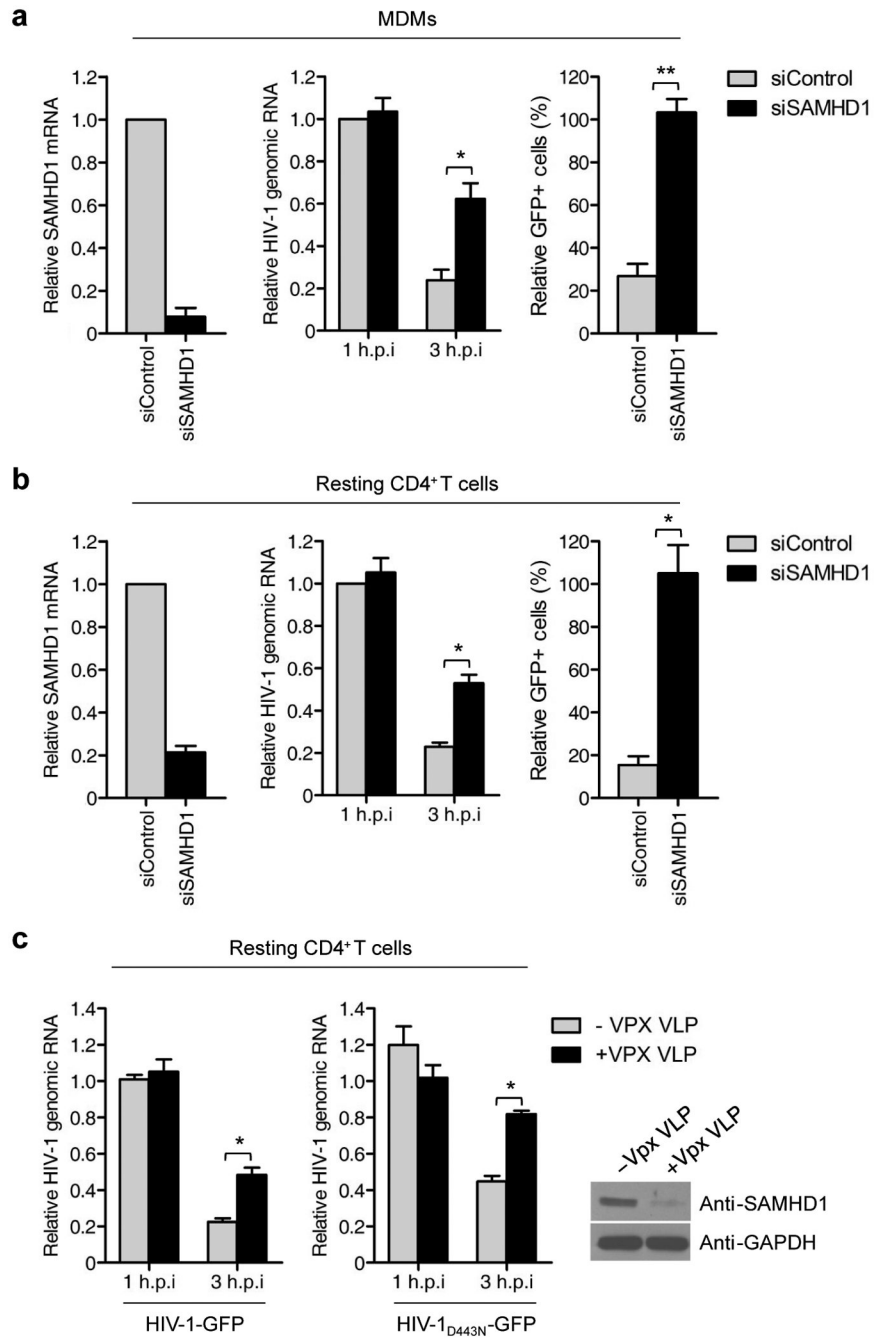
Figure 3.
SAMHD1 degrades HIV-1 RNA in primary human MDMs and CD4^{+} T cells. (**a**) CD14^{+} monocytes isolated from three donors were differentiated into MDMs. MDMs were transfected with siRNA to *SAMHD1* or control siRNA and then infected with 100 ng of HIV-1-GFP. The efficiency of *SAMHD1* knockdown was evaluated by qRT-PCR (left). Total viral RNA was quantified at the indicated times post-infection by qRT-PCR using *gfp*-specific primers. The data were normalized to an internal *β-actin* (middle). Quantification of GFP-positive cells by flow cytometry of MDMs (right). (**b**) Post-activated resting CD4^{+} T

cells from three donors were transfected with siRNA to *SAMHD1* or control siRNA and then infected with 100 ng of HIV-1-GFP. The efficiency of *SAMHD1* knockdown (left), HIV-1 RNA levels (middle) and HIV-1 infectivity (right) were analyzed as in **a**. (**c**) Effect of Vpx treatment on the HIV-1 RNA stability in resting CD4$^+$ T cells. Resting CD4$^+$ T cells were challenged with HIV-1-GFP or HIV-1-GFP$_{D443N}$ in the presence of Vpx VLP. HIV-1 RNA levels were quantified as in **a**. In **a-c**, data are presented as the mean ± s.d. of three experiments. (* and ** indicate significant differences compared with siControl or –Vpx VLP control at $P < 0.05$ and $P < 0.001$, respectively, using the two-tailed Student's t test).
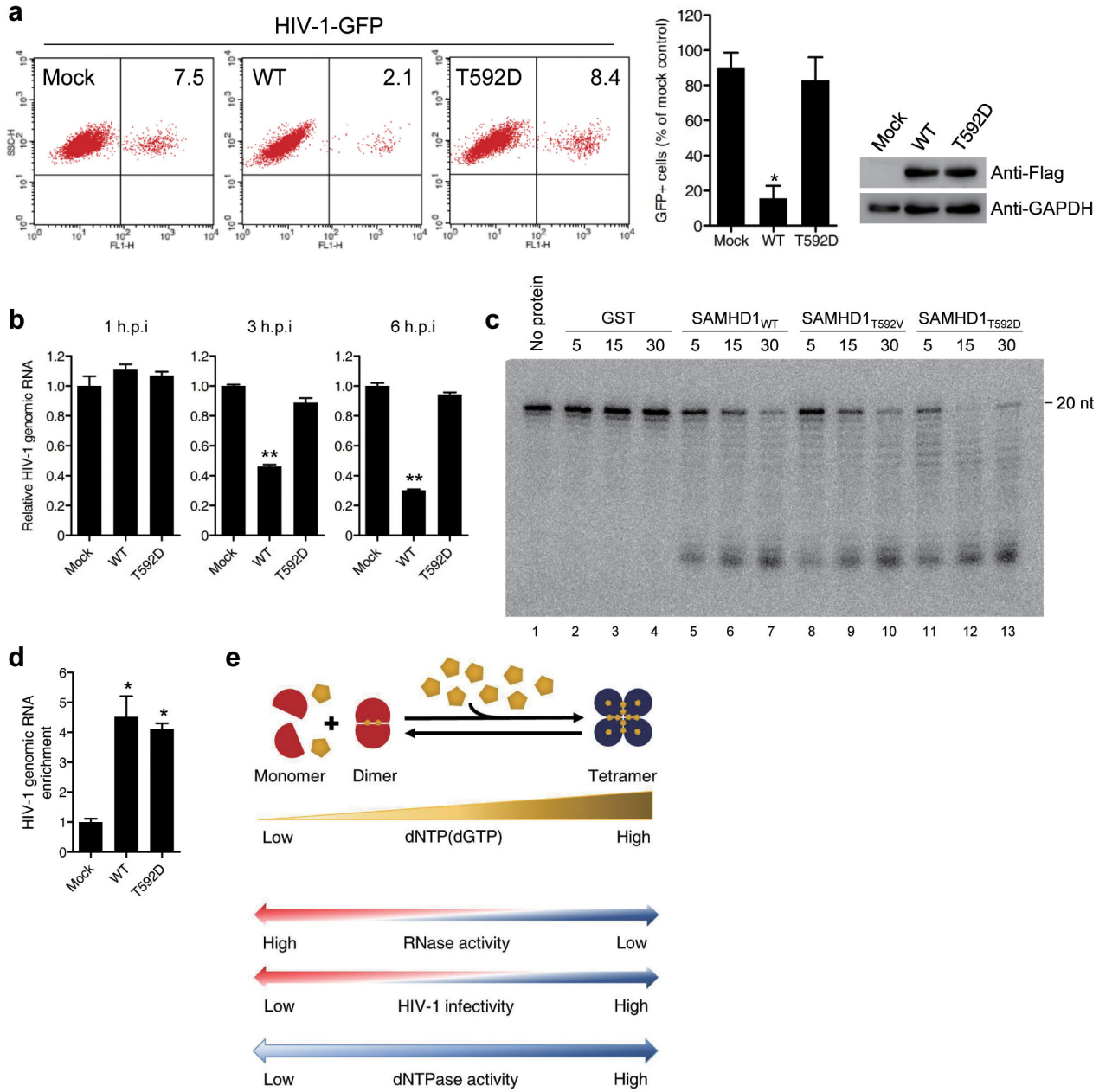
Figure 4. Phosphorylation of SAMHD1 regulates RNase activity

(**a**–**c**) U937 cells stably expressing an empty vector (mock) or Flag-tagged SAMHD1 variants were treated with PMA and infected with 100 ng of pLai envGFP3. (**a**) Flow cytometric analysis 48 hpi to measure the percentage of GFP-positive cells. The percentage of GFP-positive cells was calculated relative to the number of GFP-positive mock-transfected cells (right). Western blot analysis of cell extracts using the anti–Flag antibody. GAPDH was used as a loading control. (**b**) HIV-1 genomic RNA content was quantified by qRT-PCR using HIV-1 *gfp*-specific primers. The data were normalized to an internal *β-actin*. (**c**) Recombinant SAMHD1$_{T592V}$ and SAMHD1$_{T592D}$ proteins were purified from *E. coli*. The RNase activity assay was performed as described in Fig. 1 using 5′-end ^{32}P labeled

20-mer ssRNA substrates. (**d**) Effect of SAMHD1 T592 phosphorylation on substrate binding. RIP analysis was performed as described in Fig. 2f, except that cell lysates were immunoprecipitated using an anti-Flag antibody. In **a, b**, and **d**, data are presented as the mean ± s.d. of triplicate experiments. (* and ** indicate significant differences compared with the mock-transfected control at $P < 0.05$ and $P < 0.001$, respectively, using the two-tailed Student's t test). **e**. Model for anti-HIV-1 activity mediated by SAMHD1 RNase function.